Nonlinear Modified Concurrent Equalizer

Kayol S. Mayer, Candice Müller, Maria C. F. de Castro, and Fernando C. C. de Castro

***Abstract*—Wireless and optical communication systems not infrequently are disrupted by intersymbol interference (ISI). Wireless communications are degraded by multipath propagation in the wireless channel, while optical communications are degraded due to chromatic and polarization mode dispersion. For both cases, equalization techniques are applied to circumvent the problem. In this context, this letter proposes a novel concurrent blind equalizer, based on the nonlinear modified constant modulus algorithm (NMCMA) and on the soft direct decision (SDD) algorithm. The proposed nonlinear modified concurrent equalizer (NMCE) combines the NMCMA sharp decision regions with the SDD fast convergence, resulting in improved performance. The NMCE is compared with the NMCMA and with the constant modulus algorithm CMA-SDD equalizers under static and dynamic multipath scenarios with nonlinearities at the receiver analog front-end. Results show that the proposed solution presents lower steady-state mean squared error (MSE) and reduced symbol error rate (SER) when compared with the NMCMA and the CMA-SDD equalizers, even in dynamic propagation scenarios.**

***Index Terms*—Adaptive equalizers, Blind equalizers, Doppler effect, Multipath channels.**

I. INTRODUCTION

INTERSYMBOL interference (ISI) [1], which is essentially caused by the channel dispersion, is one of the most relevant impairment in digital wireless communication [1], [2]. ISI is not only present in wireless communications but also in coherent optical receivers due to chromatic and polarization mode dispersion [3]. Wireless and optical systems mitigate the ISI by means of channel equalization techniques [4]–[8], which basically implement the deconvolution of the channel impulse response (CIR) [1].

Though several modern communication systems are moving toward multicarrier modulation schemes to combat ISI, multicarrier solution is unfeasible to certain applications due its high peak-to-average power ratio (PAPR) [9]. High PAPR requires high power amplifier backoff to avoid the amplifier saturation, which is a problem especially for portable devices. In this context, single carrier techniques have been investigated as a potential architecture for 5g technology [10]–[12].

In single carrier systems, an adaptive equalizer is an inverse filter whose coefficients are adaptively adjusted such that the impulse response of the filter convolved with the CIR ideally results in a single impulse in some determined instant of time, achieving the so called zero-forcing (ZF) condition [1], [2].

The constant modulus algorithm (CMA) [13], in the fractionally spaced architecture, is one of the most used blind equalizers for quadrature amplitude modulation (QAM) [2]. Nevertheless, the CMA has a slow convergence rate, a moderate residual mean squared error (MSE), and it does not recover the phase of the received signal distorted by multipath [14].

In order to address these CMA issues, Oh and Chin [14] proposed a solution based on the partitioning of the Godard cost function [13] into its real and imaginary components. The modified constant modulus algorithm (MCMA) proposed by Oh and Chin solves the CMA phase recovery issue, as well as increases the convergence rate and reduces the residual MSE.

De Castro and co-workers [6] proposed another method to circumvent the CMA issues, where a concurrent architecture, composed by a CMA and a direct decision (DD) [15] equalizers, was addressed. Using as reference the work of De Castro [6], Chen replaced the DD equalizer for a soft direct decision (SDD) equalizer [4], thus achieving faster convergence rate for the CMA-SDD when compared with the CMA-DD equalizer.

In sequel, Wang proposed the nonlinear modified constant modulus algorithm (NMCMA) [16], based on a nonlinear transmittance [17]. The NMCMA achieves better results than the MCMA due to the cohesion of the decision region provided by the nonlinear sinusoidal transmittance.

Techniques equally important have been proposed, aiming to improve the performance of blind equalizers [5], [18]–[20]. In [5], the authors applied a blind fuzzy controller algorithm to increase the equalizer convergence speed and decrease the residual MSE. A different solution was proposed in [19]. Similarly to the solution proposed in [6], in [19] two equalizers are continuously running in parallel and their combination is adapted to maximize the overall performance. In [19], the soft switching between the blind and DD components is enabled by the convex combination of the components, as soon as a sufficiently low MSE level is achieved, instead of the hard decision of [6].

In such context, this work proposes a new equalization technique, based on the NMCMA and SDD algorithms, working in a modified concurrent architecture. In the proposed solution, SDD algorithm performs the soft decision and both algorithms, linear NMCMA and SDD, continuously contribute to the equalizer output by means of a nonlinear transmittance. In this way, the proposed solution combines the sharper decision regions of the NMCMA with the reduced uncertainty of the SDD decisions, achieving improved performance, even for operation in nonlinear dynamic propagation scenarios. The proposed nonlinear modified concurrent equalizer (NMCE) has been evaluated under the static channel proposed in [21]

The associate Editor coordinating the review of this manuscript and approving it for publication was professor José Cândido Silveira Santos Filho.

Kayol S. Mayer is with the Department of Communications, University of Campinas, Campinas, SP, Brazil. (e-mail: kayol@decom.fee.unicamp.br)

Maria C. F. de Castro and Fernando C. C. de Castro are with the School of Technology, Pontifical Catholic University of Rio Grande do Sul, Porto Alegre, RS, Brazil. (e-mail: cristina.felippetto@hotmail.com, fcastro@pucrs.br).

Candice Müller is with the Technology Center, University of Santa Maria, Cidade Universitária, RS, Brazil. (e-mail: candice.muller@ufsm.br).

This study was financed in part by the Coordenação de Aperfeiçoamento de Pessoal de Nível Superior – Brasil (CAPES) – Finance Code 001.

Digital Object Identifier: 10.14209/jcis.2019.21

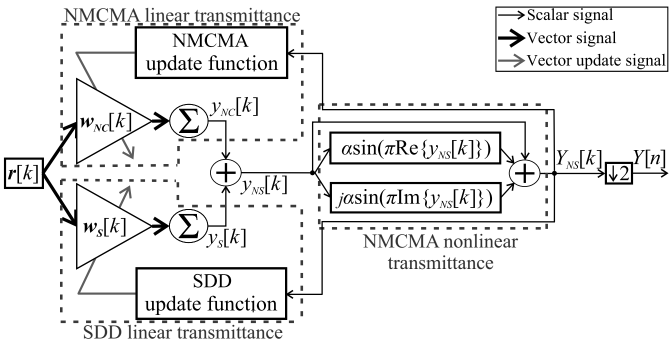

Fig. 1. Proposed NMCE architecture with NMCMA and SDD update functions given by (2) and (4), respectively.

and under the dynamic channel operation based on [21], [22]. For both cases, nonlinearities have been considered. Results show that the NMCE achieves lower steady-state MSE and reduced SER when compared with the NMCMA and the CMA-SDD equalizers.

II. Proposed Nonlinear Modified Concurrent Equalizer

Fig. 1 presents the proposed nonlinear modified concurrent equalizer. The three dashed blocks in the proposed architecture represent three signal transmittances that, operating jointly, are responsible for the NMCE increased performance. The proposed NMCE concurrent architecture combines the NMCMA linear transmittance block output $y_{NC}[k]$, responsible for the constellation phase recovery, with the SDD linear transmittance block output $y_S[k]$, which enforces the convergence process and, consequently, increases its speed. Subsequently, the NMCMA nonlinear transmittance minimizes the instant error of the equalizer output $Y_{NS}[k]$ by establishing sharper decision regions.

Notice that, in the classical CMA-DD [6] and CMA-SDD [4] concurrent architectures, the concurrent equalizer output is given simply by the linear combination of both individual equalizers. Differently, the here proposed concurrent architecture firstly linearly combines the SDD output with the NMCMA output and, in the sequence, applies this linearly combined result to the nonlinear transmittance of the NMCMA equalizer. The nonlinear transmittance can be considered as a hidden neuron of a feedforward neural network, which is given by a sinusoidal complex-valued activation function.

The proposed NMCE is a fractionally spaced equalizer (FSE) [23] with an oversampling factor of two; therefore, the time interval between two consecutive samples k and $k+1$ is $T/2$, where T is the symbol period given by $S_R = 1/T$ and S_R is the system baud rate.

The NMCE output $Y_{NS}[k]$ is given by

$$Y_{NS}[k] = y_{NS}[k]+\alpha[\sin(\pi\mathrm{Re}\{y_{NS}[k]\})+j\sin(\pi\mathrm{Im}\{y_{NS}[k]\})],$$

where $\mathrm{Re}\{\cdot\}$ and $\mathrm{Im}\{\cdot\}$ return the real and imaginary parts of their argument, respectively. $k = 0, 1, \ldots, k \to \infty$ is the FSE discrete time index for the sample rate $S_S = \Gamma S_R$, where $\Gamma = 2$ is the FSE oversampling factor. α is the nonlinear control parameter defined in the range of $[0, 1/\pi]$ [16]. For $\alpha = 0$, the NMCMA is simplified to the MCMA equalizer [14]. $y_{NS}[k]$ is the linear transmittance output of the NMCE, presented in Fig. 1, and it is obtained as

$$y_{NS}[k] = \boldsymbol{w_{NC}}[k]^T\boldsymbol{r}[k] + \boldsymbol{w_S}[k]^T\boldsymbol{r}[k],$$

where $[\cdot]^T$ denotes the vector transpose operator, $\boldsymbol{w_{NC}}[k] = [w_{NC_0}[k] \quad w_{NC_1}[k] \quad \cdots \quad w_{NC_{L_{EQ}-1}}[k]]^T$ is the vector that represents the FIR filter coefficients of the NMCMA equalizer and $\boldsymbol{w_S}[k] = [w_{S_0}[k] \quad w_{S_1}[k] \quad \cdots \quad w_{S_{L_{EQ}-1}}[k]]^T$ is the vector that represents the FIR filter coefficients of the SDD equalizer. $\boldsymbol{r}[k] = [r[k] \quad r[k-1] \quad \cdots \quad r[k-L_{EQ}+1]]^T$ is the channel regressor [6], $L_{EQ} \geq \Gamma L_{CH} - 1$ is the number of coefficients of the equalizer, and L_{CH} is the channel dispersion.

Based on [16], the update of the NMCMA coefficient vector $\boldsymbol{w_{NC}}[k]$ of the proposed architecture, is given by

$$\boldsymbol{w_{NC}}[k+1] = \begin{cases} \boldsymbol{w_{NC}}[k] - \eta_{NC}\boldsymbol{\nabla} J_{NC}[k], & \forall \text{ even } k, \\ \boldsymbol{w_{NC}}[k], & \forall \text{ odd } k, \end{cases} \tag{1}$$

where η_{NC} is the adaptive step of the NMCMA equalizer and $\boldsymbol{\nabla} J_{NC}[k]$ is the gradient vector respective to the NMCMA coefficients as

$$\boldsymbol{\nabla} J_{NC}[k] = \left[\frac{\partial J_{NC}[k]}{\partial w_{NC_0}[k]} \quad \frac{\partial J_{NC}[k]}{\partial w_{NC_1}[k]} \quad \cdots \quad \frac{\partial J_{NC}[k]}{\partial w_{NC_{L_{EQ}-1}}[k]}\right]^T,$$

being $J_{NC}[k]$ the NMCMA modified cost function:

$$J_{NC}[k] = \frac{1}{4}[(\mathrm{Re}\{Y_{NS}[k]\}^2 - \gamma_R)^2 + (\mathrm{Im}\{Y_{NS}[k]\}^2 - \gamma_I)^2],$$

where γ_R and γ_I are the real and imaginary dispersion constants, respectively, proposed in [14].

By means of (1), the update of the NMCMA coefficient vector is given by

$$\boldsymbol{w_{NC}}[k+1] = \begin{cases} \boldsymbol{w_{NC}}[k] + \eta_{NC} e_{NS}[k]\boldsymbol{r}[k]^*, & \forall \text{ even } k, \\ \boldsymbol{w_{NC}}[k], & \forall \text{ odd } k, \end{cases} \tag{2}$$

where $[\cdot]^*$ denotes the conjugate operator and $e_{NS}[k] = \mathrm{Re}\{e_{NS}[k]\} + j\mathrm{Im}\{e_{NS}[k]\}$ is the error function of the NMCMA equalizer, with real component $\mathrm{Re}\{e_{NS}[k]\} = \mathrm{Re}\{Y_{NS}[k]\}(\gamma_R - \mathrm{Re}\{Y_{NS}[k]\}^2)[1 + \alpha\pi\cos(\pi\mathrm{Re}\{y_{NS}[k]\})]$ and imaginary component $\mathrm{Im}\{e_{NS}[k]\} = \mathrm{Im}\{Y_{NS}[k]\}(\gamma_I - \mathrm{Im}\{Y_{NS}[k]\}^2)[1 + \alpha\pi\cos(\pi\mathrm{Im}\{y_{NS}[k]\})]$.

The update of the SDD coefficients $\boldsymbol{w_S}[k]$ of the proposed NMCE is based on [21], and is given as follows

$$\boldsymbol{w_S}[k+1] = \begin{cases} \boldsymbol{w_S}[k] + \eta_S\boldsymbol{\nabla} J_S[k], & \forall \text{ even } k, \\ \boldsymbol{w_S}[k], & \forall \text{ odd } k, \end{cases} \tag{3}$$

where η_S is the adaptive step of the SDD equalizer and $\boldsymbol{\nabla} J_S[k]$ is the gradient vector respective to the SDD coefficients

$$\boldsymbol{\nabla} J_S[k] = \left[\frac{\partial J_S[k]}{\partial w_{S_0}[k]} \quad \frac{\partial J_S[k]}{\partial w_{S_1}[k]} \quad \cdots \quad \frac{\partial J_S[k]}{\partial w_{S_{L_{EQ}-1}}[k]}\right]^T,$$

being $J_S[k]$ the SDD modified cost function, given by

$$J_S[k] = \rho\ln(p(Y_{NS}[k])),$$

where ρ is the SDD variance and $p(Y_{NS}[k])$ is the SDD *a posteriori* probability [4] of the nonlinear output $Y_{NS}[k]$.

TABLE I
COMPUTATIONAL COMPLEXITIES

Equalizer	Multiplications	Additions	exp(·) evaluations	sin(·) evaluations
NMCMA [16]	$8L_{EQ}+16$	$8L_{EQ}+4$	0	4
CMA-SDD [21]	$12L_{EQ}+28$	$14L_{EQ}+21$	4	0
NMCE	$12L_{EQ}+39$	$14L_{EQ}+25$	4	4

TABLE II
DYNAMIC SCENARIO: DOPPLER FREQUENCY AND INITIAL PHASE PARAMETERS

b	θ_b (rad)	f_{D_b} (Hz)	b	θ_b (rad)	f_{D_b} (Hz)	b	θ_b (rad)	f_{D_b} (Hz)	b	θ_b (rad)	f_{D_b} (Hz)	b	θ_b (rad)	f_{D_b} (Hz)
1	5.33	2.11	6	0.06	0.31	11	1.73	2.58	16	1.99	3.46	21	4.80	3.27
2	5.86	0.33	7	1.11	0.17	12	0.29	0.13	17	5.97	2.80	22	4.99	3.95
3	0.26	0.13	8	2.07	2.94	13	0.61	3.29	18	0.21	0.41			
4	0.76	0.49	9	4.43	4.67	14	5.17	3.24	19	2.75	3.16			
5	1.66	0.44	10	0.24	0.31	15	4.36	0.06	20	2.39	0.08			

Equation (3) yields to

$$\boldsymbol{w_S}[k+1] = \begin{cases} \boldsymbol{w_S}[k] + \eta_S e_S[k]\boldsymbol{r}[k]^*, & \forall \text{ even } k, \\ \boldsymbol{w_S}[k], & \forall \text{ odd } k, \end{cases} \tag{4}$$

being $e_S[k]$ the error function of the SDD

$$e_S[k] = \frac{1}{P_S[k]} \sum_{p=2i-1}^{2i} \sum_{q=2l-1}^{2l} \exp\left(-\frac{|\xi_{p,q}[k]|^2}{2\rho}\right)\xi_{p,q}[k],$$

where $\xi_{p,q}[k] = \mathcal{S}_{p,q} - Y_{NS}[k]$ is the difference between the SDD reference symbol $\mathcal{S}_{p,q}$ [4] and the NMCE equalizer output, and $P_S[k]$ is the *a posteriori* unnormalized Probability Density Function (PDF) of the SDD equalizer, given by

$$P_S[k] = \sum_{p=2i-1}^{2i} \sum_{q=2l-1}^{2l} \exp\left(-\frac{|\xi_{p,q}[k]|^2}{2\rho}\right).$$

The NMCE output $Y_{NS}[k]$ is decimated by a factor of 2 to reproduce the output $Y[n]$, being n the discrete time index so that the Sample Rate $S_S = S_R$.

Table I presents the NMCMA, CMA-SDD, and NMCE computational complexities, recalling that L_{EQ} is the number of coefficients of the equalizer. Note that the NMCE approach presents a minimally higher complexity than the CMA-SDD.

III. EXPERIMENTAL RESULTS

The proposed NMCE equalizer has been evaluated and compared with NMCMA and CMA-SDD equalizers under static and dynamic communication channels with nonlinearities at the receiver front-end. Simulations consider 256-QAM modulation scheme, baud rate of $S_R = 10$ MBd, and an upsampling factor $\Gamma = 2$, as presented in [21], in order to have a FSE architecture. The stream of symbols is generated by a pseudo random generator with uniform distribution and the upsampled symbols $s[k]$ are applied to the communication channel, where AWGN, multipath, Doppler shift effects, and nonlinearities at the receiver analog front-end are introduced.

The static channel evaluated is the one proposed by [21], which presents an impulse response with $B = 22$ complex samples. The dynamic channel is a modified version of the channel presented in [21], where each one of the B complex taps is multiplied by a sinusoid $\cos(2\pi f_{D_b} k/S_S + \theta_b)$ [22], with $1 \le b \le B$. θ_b is the b^{th} initial phase, respective to the b^{th} path, obtained randomly from an uniform distribution between $(0, 2\pi]$ rad. f_{D_b} is the b^{th} Doppler frequency, obtained randomly from an uniform distribution in the frequency intervals between $[0.05, 0.5]$ Hz and $[2.0, 5.0]$ Hz. Table II presents the $B = 22$ values of f_{D_b} and θ_b.

The received symbols at the channel output are given by

$$u[k] = \sum_{i=0}^{\Gamma L_{CH}-1} h_i[k]s[k-i] + a[k],$$

where $s[k]$ is the transmitted symbol sequence, $a[k]$ is the AWGN samples defined by the signal-to-noise ratio SNR = σ_S^2/σ_N^2, where σ_S^2 is the signal variance, σ_N^2 is the noise variance, and $h_i[k]$ is the i^{th} path of the upsampled dynamic CIR vector $\boldsymbol{h}[k] = [h_0[k] \quad h_1[k] \quad \cdots \quad h_{\Gamma L_{CH}-1}[k]]^T$. After that, based on [24], the nonlinearities at the receiver front-end are introduced as: $r[k] = u[k] + 0.01u^2[k] + 0.01u^3[k]$. The received symbols $r[k]$ are applied to the channel equalizer under test. Notice that NMCMA, NMCE, and CMA-SDD are FSE equalizers. Thus, the equalizer output is downsampled by 2. Finally, the equalized symbols $Y[n]$ and the transmitted symbols are used to determine the SER and the MSE.

The same operating conditions have been applied to NMCMA, CMA-SDD and NMCE equalizers. The number of coefficients of each equalizer is $L_{EQ} = 26$ [21]. The initialization scheme is as follows:

- The initialization of the CMA and the NMCMA filter coefficients follows the single spike method [23];
- The SDD coefficient vector starts with $\boldsymbol{w_S}[0] = \boldsymbol{0} + j\boldsymbol{0}$;
- The SDD variance is set to $\rho = 0.4$;
- The adaptive steps are $\eta_C = \eta_{NC} = 3\cdot10^{-8}$, $\eta_S = 2\cdot10^{-4}$;
- $\alpha = 0.15$ for the NMCMA and $\alpha = 0.30$ for the NMCE;
- The dispersion constants of the NMCMA are $\gamma_R = \gamma_I = 152.2$, and of the CMA is $\gamma = 237.2$.

The performance of the proposed NMCE is evaluated against CMA-SDD and NMCMA algorithms by means of the resulting SER and MSE. MSE is computed considering an

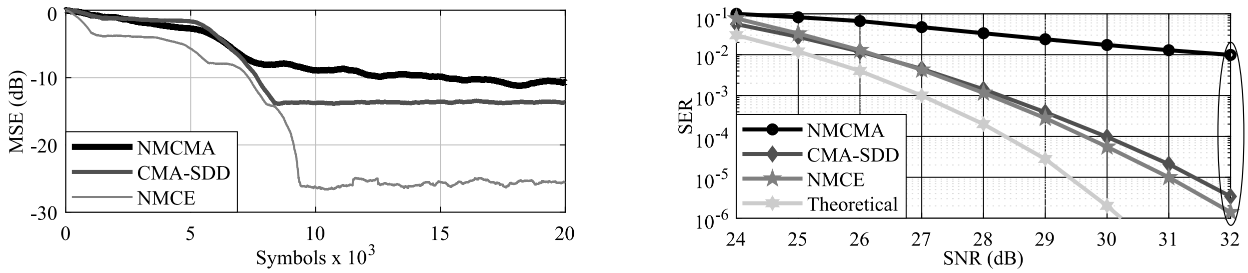

(a) (b)

Fig. 2. 256-QAM simulation results of the NMCMA, CMA-SDD and NMCE equalizers for the static channel presented in [21] with the nonlinearities at the receiver front-end [24] and the theoretical SER under an AWGN channel [25]: (a) MSE comparison, (b) SER comparison.

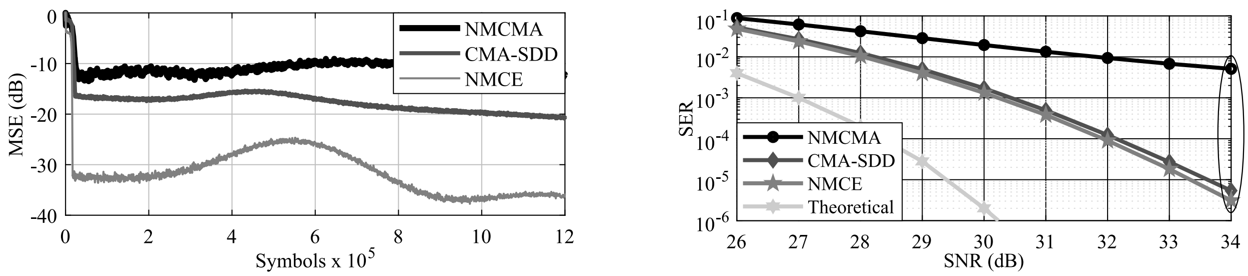

(a) (b)

Fig. 3. 256-QAM simulation results of the NMCMA, CMA-SDD and NMCE equalizers for the proposed dynamic channel based on [21], [22] with the nonlinearities at the receiver front-end [24] and the theoretical SER under an AWGN channel [25]: (a) MSE comparison, (b) SER comparison.

average window of $1,000$ symbols. The resulting MSE curve for each equalizer is averaged over 10 subsequent simulations for SNR = 60 dB. SER is computed considering 1x10^6 symbols after algorithm convergence. The resulting SER curve for each equalizer is averaged over 10 subsequent simulations for each SNR. The set of results are shown in Figs. 2 and 3.

Fig. 2 compares the results of NMCMA, NMCE, and CMA-SDD concurrent equalizers for the static multipath scenario defined in [21] and with nonlinearities based on [24]. Fig. 2a shows that the convergence of the simulated equalizers is established after 9x10^3 symbols. The NMCE presents a better performance than the NMCMA, achieving 15 dB lower for the steady-state MSE, also presenting a better performance than the CMA-SDD, achieving 11 dB lower for the steady-state MSE. For analysis purposes, Fig. 2b presents the theoretical SER limit for 256-QAM under AWGN channel [25]. NMCE presents a better performance than NMCMA and CMA-SDD, achieving 3.5 orders of magnitude lower SER and $1/2$ order of magnitude lower SER for SNR $\geq$ 32 dB, respectively.

Fig. 3 compares the results of NMCMA, NMCE, and CMA-SDD concurrent equalizers for the dynamic multipath scenario depicted in Table II, which is based on [21], [22] and with nonlinearities based on [24]. Fig. 3a shows that the convergence of simulated equalizers is established after 3x10^4 symbols. Notice that all equalizers present MSE fluctuations caused by the Doppler shifts. In Fig. 3b, the theoretical 256-QAM curve is the same presented in Fig. 2b. NMCE presents a better performance than NMCMA and CMA-SDD, obtaining 3 orders of magnitude lower SER and $1/3$ order of magnitude lower SER for SNR $\geq$ 34 dB, respectively.

IV. Conclusion

This work proposed a novel blind equalization scheme for M-QAM single carrier systems. The proposed NMCE firstly combines the linear transmittance of the NMCMA and SDD equalizers and, in the sequence, applies this linearly combined result to the nonlinear transmittance of the NMCMA equalizer, resulting in a modified concurrent architecture. The proposed architecture is able to (1) to recover the constellation phase, (2) to minimize the MSE and (3) to reduce the SER.

The performance of the proposed approach is compared with the NMCMA and the state of the art CMA-SDD concurrent equalizer under static and dynamic multipath scenarios with nonlinearities at the receiver analog front-end.

The proposed concurrent architecture proved to be robust under static and dynamic channels, achieving faster convergence rate and reduced steady-state MSE when compared with NMCMA and with CMA-SDD equalizers. For the static channel, NMCE presented SER values up to 3 orders of magnitude better than the NMCMA equalizer and up to $1/2$ order of magnitude better than the CMA-SDD equalizer. Under dynamic multipath channel, with Doppler shift present in all respective paths, NMCE achieves reduced steady-state MSE when compared with the NMCMA and CMA-SDD equalizers. As for the SER, the results obtained with NMCE are up to 3 orders of magnitude better than the NMCMA equalizer and $1/3$ order of magnitude better than the CMA-SDD equalizer.

Future work will address (1) the evaluation of a convex combination instead of the SDD algorithm; (2) the use of additional techniques to adapt the algorithms step-size; and (3) the viability of applying the NMCE to optical communications.

REFERENCES

[1] S. Haykin, *Digital Communication Systems*, 1st ed. Wiley, 2013, ISBN: 978-0471647355.

[2] J. G. Proakis and M. Salehi, *Digital Communications*, 5th ed. New York: McGraw-Hill, 2008, ISBN: 978-0072957167.

[3] E. Ip and J. M. Kahn, "Digital equalization of chromatic dispersion and polarization mode dispersion," *Journal of Lightwave Technology*, vol. 25, no. 8, pp. 2033–2043, 2007, DOI: 10.1109/JLT.2007.900889.

[4] S. Chen, "Low complexity concurrent constant modulus algorithm and soft decision directed scheme for blind equalisation," *IEE Proceedings - Vision, Image, and Signal Processing*, vol. 150, no. 5, p. 312, 2003, DOI: 10.1049/ip-vis:20030619.

[5] K. S. Mayer, M. S. De Oliveira, C. Müller *et al.*, "Blind fuzzy adaptation step control for a concurrent neural network equalizer," *Wireless Communications and Mobile Computing*, vol. 2019, pp. 1–11, 2019, DOI: 10.1155/2019/9082362.

[6] F. C. C. De Castro, M. C. F. De Castro, and D. S. Arantes, "Concurrent blind deconvolution for channel equalization," in *ICC 2001. IEEE International Conference on Communications. Conference Record (Cat. No.01CH37240)*, vol. 2. IEEE, 2001, pp. 366–371, DOI: 10.1109/ICC.2001.936964.

[7] T. Pfau, S. Hoffmann, and R. Noe, "Hardware-efficient coherent digital receiver concept with feedforward carrier recovery for M-QAM constellations," *Journal of Lightwave Technology*, vol. 27, no. 8, pp. 989–999, 2009, DOI: 10.1109/JLT.2008.2010511.

[8] M. P. Yankov, E. P. da Silva, F. Da Ros *et al.*, "Experimental analysis of pilot-based equalization for probabilistically shaped WDM systems with 256QAM/1024QAM," in *2017 Optical Fiber Communications Conference and Exhibition (OFC)*. IEEE, 2017, pp. 1–3.

[9] N. Lahbabi, S. S. K. C. Bulusu, J. F. Hélard *et al.*, "Very efficient tone reservation PAPR reduction fully compatible with ATSC 3.0 standard: performance and practical implementation analysis," *IEEE Access*, vol. 6, pp. 58 355–58 372, 2018, DOI: 10.1109/ACCESS.2018.2874797.

[10] T. Li and M. Torlak, "Performance of ZF linear equalizers for single carrier massive MIMO uplink systems," *IEEE Access*, vol. 6, pp. 32 156–32 172, 2018, DOI: 10.1109/ACCESS.2018.2841032.

[11] W. Huang, Y. Huang, R. Zhao *et al.*, "Wideband millimeter wave communication: single carrier based hybrid precoding with sparse optimization," *IEEE Transactions on Vehicular Technology*, vol. 67, no. 10, pp. 9696–9710, 2018, DOI: 10.1109/TVT.2018.2861903.

[12] S. Buzzi, C. D'Andrea, T. Foggi *et al.*, "Single-carrier modulation versus OFDM for millimeter-wave wireless MIMO," *IEEE Transactions on Communications*, vol. 66, no. 3, pp. 1335–1348, mar 2018, DOI: 10.1109/TCOMM.2017.2771334.

[13] D. Godard, "Self-recovering equalization and carrier tracking in two-dimensional data communication systems," *IEEE Transactions on Communications*, vol. 28, no. 11, pp. 1867–1875, nov 1980, DOI: 10.1109/TCOM.1980.1094608.

[14] K. N. Oh and Y. O. Chin, "Modified constant modulus algorithm: blind equalization and carrier phase recovery algorithm," in *Proceedings IEEE International Conference on Communications ICC '95*, vol. 1. IEEE, 1995, pp. 498–502, DOI: 10.1109/ICC.1995.525219.

[15] O. Macchi and E. Eweda, "Convergence analysis of self-adaptive equalizers," *IEEE Transactions on Information Theory*, vol. 30, no. 2, pp. 161–176, mar 1984, DOI: 10.1109/TIT.1984.1056896.

[16] D. Wang, "A nonlinear modified constant modulus algorithm for blind equalization," in *CCECE 2010*. IEEE, may 2010, pp. 1–4, DOI: 10.1109/CCECE.2010.5575240.

[17] C. You and D. Hong, "Nonlinear blind equalization schemes using complex-valued multilayer feedforward neural networks," *IEEE Transactions on Neural Networks*, vol. 9, no. 6, pp. 1442–1455, 1998, DOI: 10.1109/72.728394.

[18] J. M. Filho, M. D. Miranda, and M. T. M. Silva, "A regional multimodulus algorithm for blind equalization of QAM signals: introduction and steady-state analysis," *Signal Processing*, vol. 92, no. 11, pp. 2643 – 2656, Nov 2012, DOI: 10.1016/j.sigpro.2012.04.010.

[19] M. T. M. Silva and J. Arenas-Garcia, "A soft-switching blind equalization scheme via convex combination of adaptive filters," *IEEE Transactions on Signal Processing*, vol. 61, no. 5, pp. 1171 – 1182, Mar 2013, DOI: 10.1109/TSP.2012.2236835.

[20] J. Arenas-Garcia, L. A. Azpicueta-Ruiz, M. T. M. Silva *et al.*, "Combinations of adaptive filters: performance and convergence properties," *IEEE Signal Processing Magazine*, vol. 33, no. 1, pp. 120 – 140, Jan 2016, DOI: 10.1109/MSP.2015.2481746.

[21] S. Chen and E. S. Chng, "Concurrent constant modulus algorithm and soft decision directed scheme for fractionally-spaced blind equalization," in *2004 IEEE International Conference on Communications (IEEE Cat. No.04CH37577)*, vol. 4, no. c. IEEE, 2004, pp. 2342–2346 Vol.4, DOI: 10.1109/ICC.2004.1312937.

[22] M. Ghosh, "Blind decision feedback equalization for terrestrial television receivers," *Proceedings of the IEEE*, vol. 86, no. 10, pp. 2070–2081, 1998, DOI: 10.1109/5.720253.

[23] T. J. Endres, "Equalizing with fractionally-spaced constant modulus and second-order-statistics blind receivers," Ph.D. Thesis, Cornell University, 1997.

[24] A. T. Al-Awami, A. Zerguine, L. Cheded *et al.*, "A new modified particle swarm optimization algorithm for adaptive equalization," *Digital Signal Processing*, vol. 21, no. 2, pp. 195 – 207, 2011, DOI: 10.1016/j.dsp.2010.05.001.

[25] J. R. Barry, E. A. Lee, and D. G. Messerschmitt, *Digital Communication*, 3rd ed. Norwell: Springer, 2003, ISBN: 978-1461502272.

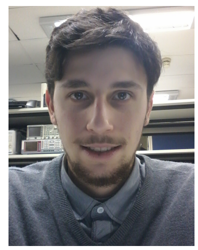

Kayol Soares Mayer received the B.Sc. degree in Automation and Control Engineering from the Pontifical Catholic University of Rio Grande do Sul - PUCRS, in 2016, and the M.Sc. degree in Electrical Engineering, also from PUCRS, in 2018. Currently, he is a Ph.D. student in Electrical Engineering at the University of Campinas - Unicamp. His current research interests include wireless and optical communications, adaptive digital signal processing, and machine learning.

Candice Müller received the B.Sc. degree in Electronics Engineering from Feevale University, in 2006, and the Ph.D. in Electrical Engineering from University of Genoa, in 2012. Currently she is adjunct professor in the Department of Electronics and Computing of Federal University of Santa Maria, Brazil. Her research interests include digital communication systems, adaptive digital signal processing, and antennas.

Maria C. F. de Castro received the B.Sc. degree in Electrical Engineering from Pontifical Catholic University of Rio Grande do Sul - PUCRS, Brazil, in 1983, the M.Sc. Degree in Electrical Engineering from PUCRS in 1996 and the Ph.D. in Electrical Engineering from University of Campinas, in 2001. Until 2018 she has been full professor in Electronics and Telecommunication at the Faculty of Engineering of the PUCRS, and researcher at Wireless Technologies Research Center from PUCRS. Her research interests include digital communication systems, adaptive DSP, antennas, and cognitive radio.

Fernando C. C. de Castro received the B.Sc. degree in Electrical Engineering from Pontifical Catholic University of Rio Grande do Sul - PUCRS, Brazil, in 1983, the M.Sc. Degree in Electrical Engineering from PUCRS in 1995 and the Ph.D. in Electrical Engineering from University of Campinas, in 2001. Currently he is full professor in Electronics and Telecommunication at the Faculty of Engineering of the PUCRS, and scientific coordinator at Wireless Technologies Research Center from PUCRS. His research interests include digital communication systems, adaptive DSP, antennas, electromagnetics, and cognitive radio.